JOURNAL OF MATERIALS SCIENCE **34** (1999) 6177–6182

Granular and intergranular properties of hot pressed BSCCO (2223) superconductors

A. TAMPIERI
IRTEC-CNR, via Granarolo, 64 Faenza, Italy
E-mail: tampieri@irtec1.irtec.bo.cnr.it

D. FIORANI
ICMAT-CNR, Area della Ricerca di Roma C.P. 10, 00016 Monterotondo stazione, Roma, Italy

N. SPARVIERI
Alenia Ricerche. via Tiburtina, Roma, Italy

S. RINALDI
Università di Ancona, Dip.Scienze dei Materiali e della Terra, via Brecce Bianche, Ancona, Italy

G. CELOTTI
IRTEC-CNR, via Granarolo, 64 Faenza, Italy

R. BARTOLUCCI
Università di Ancona, Dip.Scienze dei Materiali e della Terra, via Brecce Bianche, Ancona, Italy

The effect of hot pressing conditions (sintering temperature and time) on the superconducting properties of (2223) Bi(Pb)SrCaCuO were investigated by transport and magnetic measurements. The advancement of the densification process leads first to an improvement of the electrical connectivity between grains ($J_{c\,transport}$ increases) and then to a deterioration of both intragranular and intergranular properties (T_c, $J_{c\,magnetic}$ and $J_{c\,transport}$ decrease) because of the induced loss of oxygen, 2212 continuous intergrain network and other defect formation.

1. Introduction

In view of technological applications of high T_c superconductor [1] an important task is to obtain dense and textured materials, maintaining a good control of grain boundary characteristics (crystallographic phases, defects, oxygen content) in order to optimize the electrical connectivity between grains [2–7]. However, effective densification processes, like hot-pressing, have been found from one side to promote complete densification and oriented texture, but on the other side to induce partial melting phenomena with recrystallization of secondary phases. Because of diffusion processes at grain boundary, they tend to form a continuous layer around grains and compact, well structured intergrain areas. As a matter of fact, even if the grains are tightly connected and well oriented, the actual transport current decreases [8].

In order to enlighten the relationship linking microstructural and functional properties of BSCCO superconductors, we have prepared dense and textured samples and investigated the effect of hot pressing conditions (sintering temperature and time) by transport and magnetic measurements.

2. Experimental

Bulk Bi(Pb)SrCaCuO (2223) materials were prepared starting from a powder obtained by solid-state reaction of oxides and carbonates with the nominal composition $Bi_{1.84}Pb_{0.34}Sr_{1.91}Ca_{2.03}Cu_{3.06}O_X$. Powder was uniaxially pressed at 150 MPa and the pellets obtained were hot-pressed using an "Instron" apparatus adequately fitted for the experiments. The alumina die and plungers were sputtered with silver in order to prevent the reaction of the superconductor with alumina. The constant pressure of 7 MPa was applied before heating. The hot-pressing temperature was reached with a heating rate of 10 °C/min. Different sintering temperatures and times were used in the range 790–810 °C and 2–6 h, respectively (Table I). Details on powder preparation, hot-pressing technique and relative theories were described in previous papers [9, 10].

X-ray diffraction (XRD) data were taken at room temperature with graphite monochromatized CuK_α radiation. The relative amounts of different phases of BSCCO system (2201, 2212, 2223) were evaluated by using the intensity ratio of the principal peaks falling in similar angular ranges. The degree of grain orientation

TABLE I Sintering conditions and samples characteristics

Sample code	Sintering temperature (°C)	Sintering time (h)	Relative density (%)	Orientation factor (%)	2223/2212 (vol %)	$T_{c\,onset}$ (K)	$T_{c\,offset}$ (K)	J_{ct} (A/cm^2)	J_{cm} 77 K, $H = 0$ A/m (A/cm^2)	J_{cm} 5 K, $H = 800$ A/m (A/cm^2)
A	790	2	92	37	92/8	108	94	0.5	$9 \cdot 10^3$	$1.2 \cdot 10^4$
B	800	2	93	43	89/11	108	98	6	$2 \cdot 10^3$	$2.6 \cdot 10^4$
C	810	3	96	46	93/7	108	90	3	$2 \cdot 10^3$	$1.2 \cdot 10^4$
D	810	4	97	62	98/2	95	85	3	$1 \cdot 10^3$	$4.7 \cdot 10^4$
E	810	6	98	57	95/5	92	88	1	—	$7.5 \cdot 10^3$
D*	810	4	97	42	92/8	110	104	20	$6 \cdot 10^3$	$5.3 \cdot 10^4$

*= Recovered 47 h at 840 °C in fluent air.

in the axial direction "F" was determined by means of XRD analysis from the Lotgering relationship, using for comparison a randomly oriented powder pattern. The value was obtained by averaging that one taken on the surface and that one in the core of the sample.

The bulk density was measured by the Archimedes' method. The morphology of the samples was investigated by means of scanning electron microscopy (Leica Cambridge Ltd.) Energy dispersion analysis X-ray (EDAX) system was also employed on the polished surfaces of sintered samples; electron probe microanalysis was performed to determine the composition of the superconducting and impurity phases. Samples were prepared by grinding on SiC abrasive paper and subsequent polishing with diamond paste up to 0.5 μm.

The superconducting properties were investigated by means of transport and magnetic measurements. The resistivity was measured by the four-probe method, with Ag-paste contacts and with a maximum feeding current of 1 mA perpendicular to the hot-pressing direction. The critical temperature was extracted from the ρ vs. T curves. Two values are deduced (Table I), i.e. the onset superconducting temperature $T_{c\,onset}$ and the zero-resistivity temperature $T_{c\,offset}$. Transport critical current (J_{ct}) was determined by I-V measurements at 77 K and zero magnetic field with voltage criterion of 1 μV/cm.

Magnetization measurements were performed by a vibrating-sample magnetometer ($77 < T < 300$ K; $H_{max} = 1.0$ T) and a SQUID magnetometer ($2 < T < 400$ K; $H_{max} = 5.5$ T) applying the field perpendicular to the pellet plane. The magnetic critical current (J_{cm}) was estimated at 5 and 77 K from the hysteresis cycles by using the Bean critical-state model.

The real and imaginary components χ' and χ'' of the internal complex ac magnetic susceptibility were measured as a function of temperature ($50 < T < 120$ K). Data were collected at a fixed frequency ($f = 1000$ Hz) for different driving fields ($0.4 \leq H_{ac} \leq 800$ A/m). Calibration has been performed using a $Gd_2(SO_4)_3 \cdot 8H_2O$ standard. Demagnetization effects have been taken into account to calculate the internal susceptibility.

3. Results

3.1. Microstructure

Table I shows that the density of the hot-pressed samples increases with sintering temperature and time. The time effect is smaller, although it shows a deep influence on the orientation factor F; indeed samples fired at 810 °C for a time longer than 2 h show an increase in the F value up to $F = 62\%$.

The volume fraction of 2212 phase changes with sintering conditions. It is worth mentioning that the starting powder had an average 2212 volume fraction around 5%, while the hot-pressing treatments cause an increase in such a value up to a maximum of 11%; on the contrary, by increasing the sintering time, the amount of this phase decreases, reaching a minimum of 2% and then increases again (see Table I for $T_s = 810$ °C).

The increase of sintering temperature, up to 800 °C and of sintering time produces an increase of both a and c cell parameters (e.g. $T_s = 790$ °C and $t_s = 2$ h : $a = 5.408$, $c = 37.14$ A; $T_s = 800$ °C and $t_s = 2$ h : $a = 5.412$, $c = 37.18$ A) ($T_s = 810$ °C and $t_s = 3$ h : $a = 5.414$, $c = 37.20$ A; $T_s = 810$ °C and $t_s = 6$ h : $a = 5.416$, $c = 37.24$ A). This should be due to the decrease of oxygen content in the inner part of the sample, induced by the advancement of the densification process, and resulting in a weaker coupling between Cu–O layers. For sintering temperatures above 800 °C the loss of oxygen becomes so important that the cell parameters decrease ($T_s = 820$ °C and $t_s = 2$ h : $a = 5.405$, $c = 37.08$ A). It is interesting to note that the c values for 2212 phase (present as impurity) behave very similarly to those of (2223) phase. For a more detailed discussion of microstructural features of the tested samples, see [8].

3.2. Transport measurements

Resistivity vs. temperature curves for samples A and B, sintered for 2 h at 790 and 800 °C respectively are reported in Fig. 1a. The increasing of the sintering temperature (T_s) for the same sintering time (t_s), does not change $T_{c\,onset}$, whereas it leads to an increase of $T_{c\,offset}$ and of the transport critical current J_{ct} (Table I). By increasing t_s at $T_s = 810$ °C (samples C, D, E) both $T_{c\,onset}$ (Fig. 1b) and J_{ct} decrease (for $t_s = 6$ h).

A further annealing in fluent air for 47 h at 840 °C on the sample D leads to an increase of both T_c and J_{ct} (sample D*) (Table I).

3.3. Magnetic measurements

A typical hysteresis cycle is reported in Fig. 2. The intragrain critical current (J_{cm}) was estimated using the Bean critical state model. J_{cm} ($H = 8 \times 10^2$ A/m) at $T = 5$ K increases with T_s for the same t_s (2 h) (samples A and B) and with t_s for the same T_s (810 °C) (samples C, D and E) (Table I). On the other hand, J_{cm} ($H = 0$) at $T = 77$ K decreases with T_s as well as with

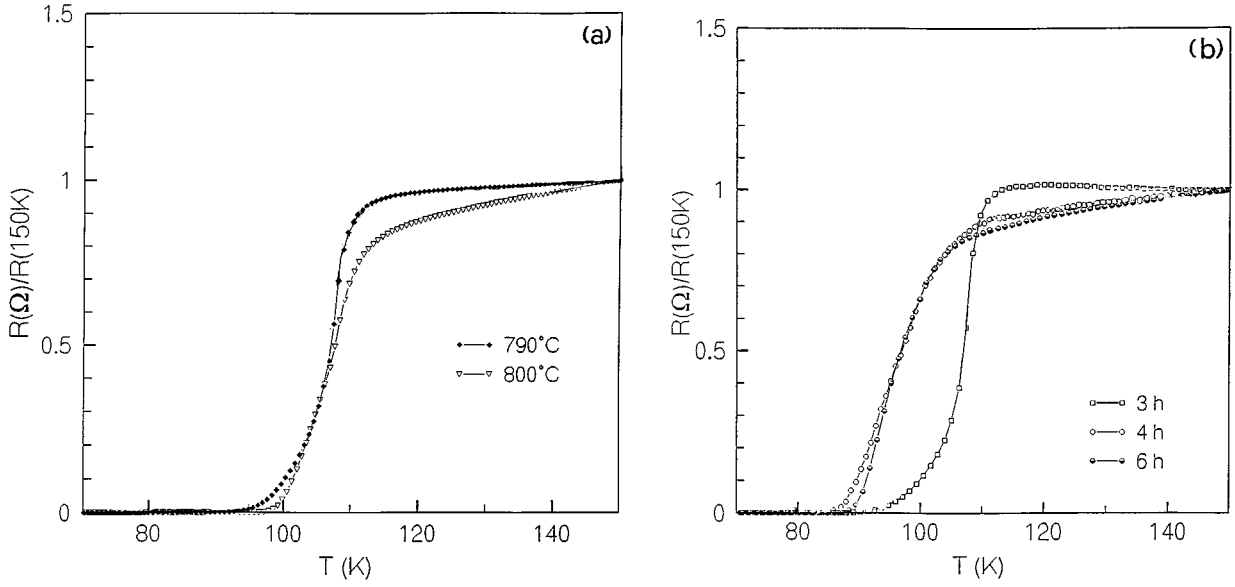

Figure 1 Resistivity vs. temperature for hot pressed samples: (a) isochronous treatments at $t_s = 2$ h ($T_s = 790\,^{\circ}$C: sample A; $T_s = 800\,^{\circ}$C: sample B), (b) isothermal treatments at $T_s = 810\,^{\circ}$C ($t_s = 3$ h: sample C; $t_s = 4$ h: sample D; $t_s = 6$ h: sample E). Resistance values are normalized at 150 K.

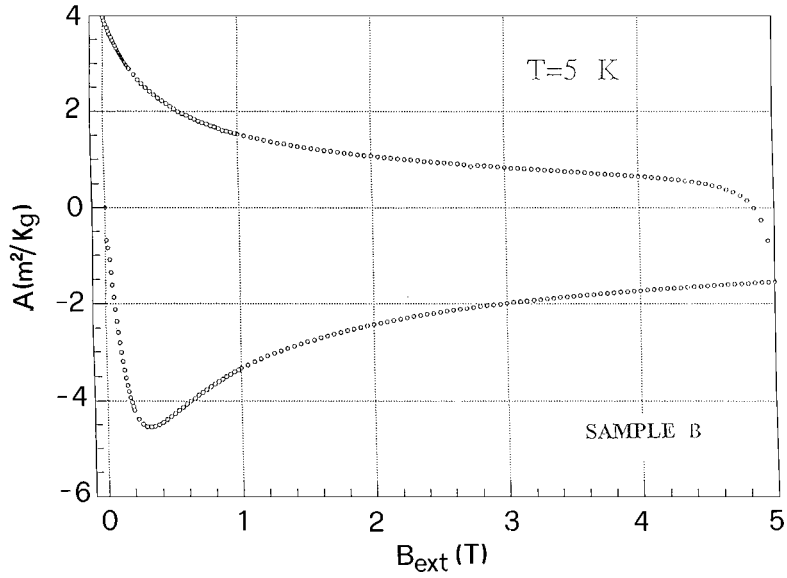

Figure 2 Hysteresis cycles at $T = 5$ K for sample B (Table I).

t_s. Reannealing in fluent air (sample D*) leads to an increase of J_{cm}.

The results of ac susceptibility measurement, (χ' and χ'' vs. T) for the samples D and D* are reported in Fig. 3. Different transitions are detected in correspondence of χ' drops. In sample D both 2223 and 2212 phases are detected, whereas for sample D* only the 2223 one. The intragranular transition temperatures T_c, below which flux is excluded by individual grains, is actually field independent in the explored field range. On the other hand, the intergranular transition temperature ($T_{c\,interg.}$), below which electrical connectivity between grains is established and flux is excluded by the whole assembly of coupled grains, is strongly field dependent, decreasing with increasing H_{ac} (Fig. 4).

4. Discussion

The results of both transport and magnetic measurements allows us to investigate the effect of hot pressing conditions on the intragranular as well as intergranular properties of BSCCO superconductors. The variation of sintering temperature and time produces microstructural changes and modifies oxygen content, density, degree of grain orientation, relative percentage of 2223 and 2212 phases and their location, which all strongly affect the superconducting properties [11].

Let's discuss first the effect on the intragranular properties, i.e. on $T_{c\,onset}$ and J_{cm}. In oxide superconductors T_c, depending on the number of charge carriers, is closely related to the fraction of oxygen vacancies [12]. T_c is known to peak generally with the oxygen content and then to decrease again as the sample becomes over-oxygenated. Since the densificstion process, responsible for the increase of the c lattice parameter, leads to a decrease of oxygen content, the decrease of T_c with increasing t_s at $T_s = 810\,^{\circ}$C indicates that the sample are in the ascending part of the T_c vs. oxygen content curve (they tend to be under-oxygenated).

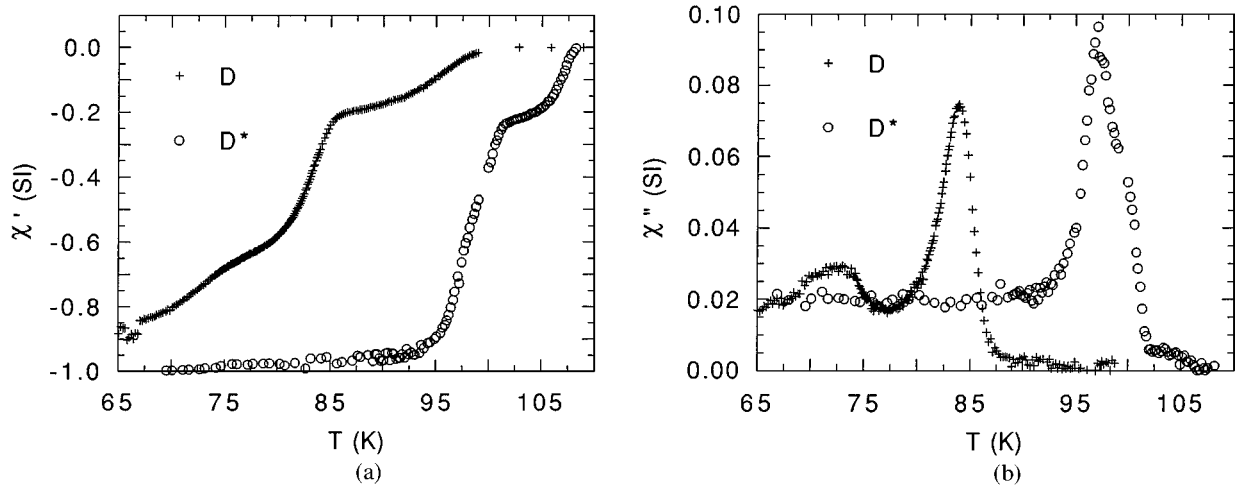

Figure 3 Temperature dependence of χ' (a) and imaginary component χ'' (b) of the ac-susceptibility for samples D and D* ($H_{ac} = 0.4$ A/m).

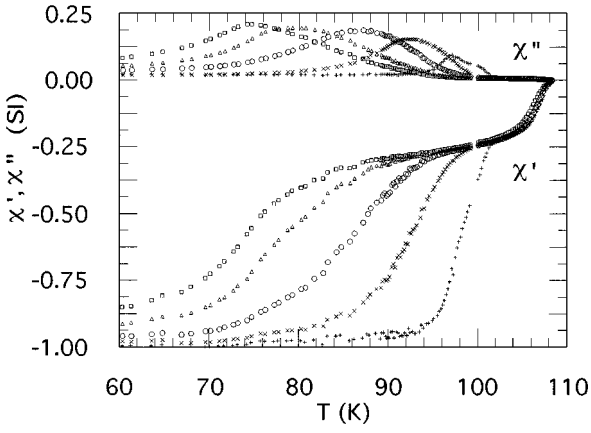

Figure 4 χ' and χ'' vs. temperature at different ac fields (+: 0.4 A/m, ×: 50 A/m, ○: 200 A/m, △: 660 A/m, □: 800 A/m) for sample D*.

The J_{cm} variation reflects the effect of sintering temperature and time on the actual pinning centers and on their strength. The different trend with T_s and t_s exhibited by J_{cm} at 5 K and at 77 K can be understood in terms of different effective pinning centers acting at low and at high temperature. At low temperature (e.g. 5 K), oxygen vacancies in the Cu–O planes are known to be effective in pinning flux lines. Such vacancies act as weak pinning centers but, because of their high number, actually they are relevant in determining the J_c value, as long as the thermal energy is very low [12]. The increase of J_{cm} at 5 K (Table I) with T_s and t_s can be explained by the increase of oxygen vacancies, determined by the increase of relative density, in agreement with the decrease of T_c. However, for long sintering times ($t_s = 6$ h at $T_s = 810\,^{\circ}$C) (sample E) J_{cm} decreases, revealing a degradation of superconducting properties, due to a heavy lack of oxygen and probably reinforced by the formation of structural defects, like microcracks (Fig. 5).

At higher temperature (e.g. 77 K) the oxygen vacancies are no longer effective as pinning centers and the dominant role on J_{cm} and on its field dependence is played by the coupling between Cu–O planes, i.e. by the actual dimensionality of the flux line lattice [13]. The loss of oxygen with increasing density, determining an increase of *c* lattice parameter, makes weaker the coupling between Cu–O planes and reduces J_c (Fig. 6). Restoring the oxygen content (e.g. by reannealing in fluent air, like for sample D*), both T_c (the transition becomes sharper and the resistivity tail becomes smaller) and J_{cm} ($T = 77$ K) strongly increase again.

The changes produced by T_s and t_s on the intergranular properties are monitored by the variation of J_{ct} (Table I). The strong increase of J_{ct} with T_s for $t_s = 2$ h (samples A and B) is clearly due to the increase of density and orientation factor, making stronger the intergranular coupling.

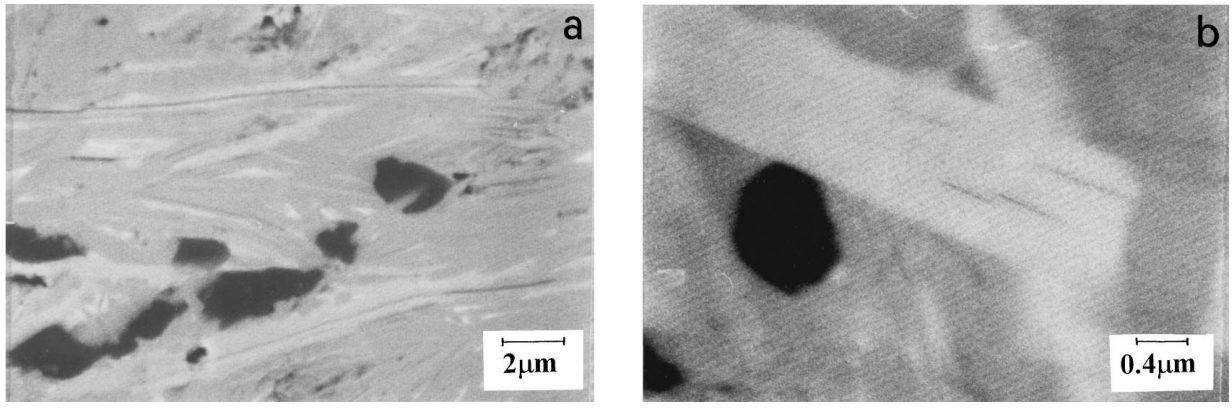

Figure 5 SEM micrographs showing microcracks in (a) grain boundary regions and (b) within the grains in sample E.

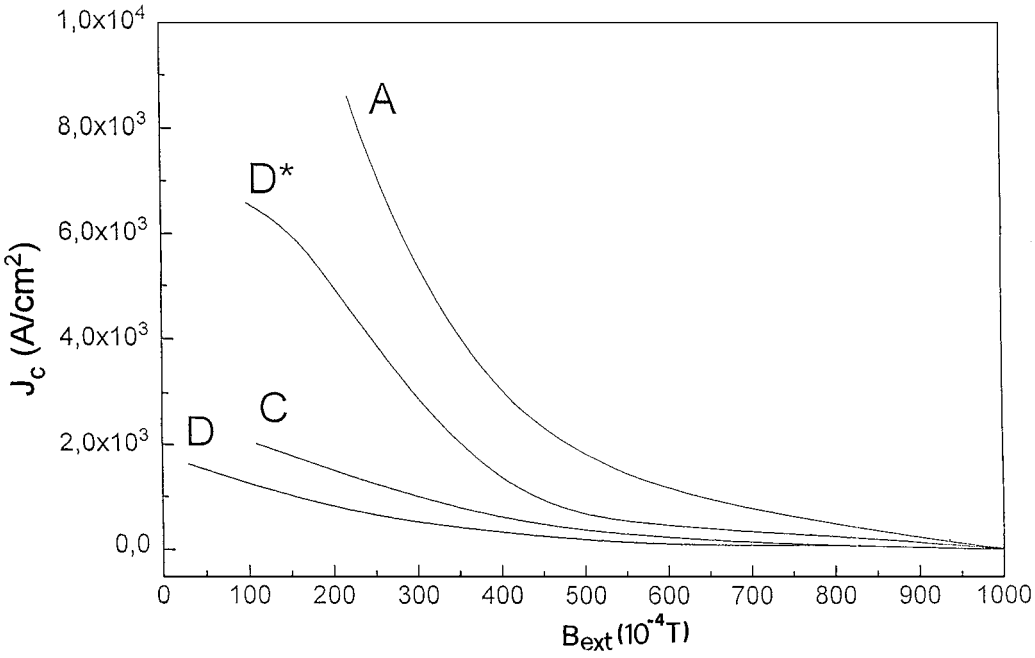

Figure 6 J_c vs. applied magnetic field at 77 K for hot-pressed samples.

However, the increase of the sintering time at 810 °C (samples C, D and E) leads to a decrease of J_{ct} (for $t_s = 6$ h). Moreover, long sintering times yield broadening in the resistivity drop at T_c. Both the decrease of J_{ct} and the broadening phenomenon reveal a lower connectivity among grains, mainly due to the organization of the 2212 phase as a continuous network at grain boundaries acting as unavoidable barrier (Fig. 5).

The effect of reannealing in fluent air (sample D*) restoring the oxygen content, reduced by the densification process, leads to an improvement of the intergranular properties, as shown by the strong increase of J_{ct} (Table I).

The higher connectivity between grains in the sample D*, although the orientation factor is lower than in sample D (Table I), is also well evidenced by ac-susceptibility measurements performed at different driving fields. For D*, $T_{c\,inter}$ is higher and decreases with H_{ac} slower than for the sample D. Although the fraction of the 2212 phase is higher in D* than in D, the associated superconducting transition is not observed in the first sample but in the latter one (Fig. 3). This fact suggests a different distribution of the 2212 phase in the two samples [14]. In sample D the 2212 phase is likely located at grain boundaries, strongly affecting the intergranular properties. On the other hand, in the sample D* the 2212 phase is likely confined in clusters under the thrust of grains randomization movement occurred during the thermal treatment of the restoring and therefore it is more easily bypassed.

5. Conclusions

We have investigated the effect of hot pressing conditions on the superconducting properties of BSCCO materials. The results show that microstructural changes, induced by the advancement in densification process (by increasing sintering temperature and time) strongly affect the superconducting intergranular and intragranular properties.

By increasing density and orientation factor, as T_s and t_s increase, J_{ct} first increases and then decreases, because of the densification-induced loss of oxygen and microcracks formation.

The presence of a fraction of 2212 phase (changing from 2% to 11% according to the sintering conditions) and mainly its distribution within the material also is greatly affected by sintering methodology and has a great influence on the electrical connectivity between the 2223 grains. Indeed, it is found that hot pressing stimulates the recrystallization of 2212 which concentrates at grain boundary and, reducing porosity and increasing the compactness of grain boundary regions, it weakens the links among the grains. Consequently, even if the fraction of 2212 is low and the orientation factor is high, J_{ct} decreases (e.g. sample B in comparison with sample D).

The intragranular properties are found to be strongly dependent on the oxygen content. Indeed, they deteriorate when the loss of oxygen becomes important with the advancement of the densification process, as shown by the decrease of T_c and J_{cm}. Restoring the oxygen content by a further annealing in air (e.g. in sample D*) both T_c and J_{cm} increase again.

References

1. A. GERBER, *Appl. Supercond.* **1** (1993) 985.
2. I. D. LUZYANIN, S. L. GINZBURG, V. P. KHAVRONIN, E. G. TAROVIK, B. LIPPOLD, J. HERRMANN, H. BORNER and M. WURLITZER, *Supercond. Sci. Technol.* **6** (1993) 597.
3. WAI LO, D. N. ZHENG, B. A. GLOWACKI and A. M. CAMPBELL, *J. Mater. Sci.* **29** (1994) 3897.
4. J. G. NOUDEM, J. BEILLE, D. BOURGAULT, A. SULPICE and R. TOURNIER, *Physica C* **230** (1994) 42.
5. W. PACHLA, P. KOVAC, H. MARCINIACK, F. GOMORY, I. HUSEK and I. POCHABA, *ibid.* **248** (1995) 29.

6. N. MURAYAMA and J. B. VANDER SANDE, *ibid.* **241** (1995) 235.
7. D. BERLING, J. BEILLE, B. LOEGEL, A. MEHDAOUI, J. G. NOUDEM and R. TOURNIER, *Supercond. Sci. Technol.* **9** (1996) 205.
8. G. CELOTTI, A. TAMPIERI, R. MASINI and M. C. MALPEZZI, *Physica C* **225** (1994) 346.
9. A. TAMPIERI, R. MASINI, L. DIMESSO, S. GUICCIARDI and M. C. MALPEZZI, *Jpn. J. Appl. Phys.* **32** (1993) 4490.
10. A. TAMPIERI and G. N. BABINI, *ibid.* **30** (1991) L1163.
11. A. OOTA, H. NOJI and K. OHBA, *Phys. Rev. B* **43** (1991) 10455.
12. D. B. MITZI, L. W. LOMBARDO and A. KAPITULNIK, *ibid.* **41** (1990) 6564.
13. G. BALESTRINO, D. V. LIVANOV, E. MILANI, B. CAMAROTA, D. FIORANI and A. M. TESTA, *ibid.* **50** (1994) 3446.
14. R. B. GOLDFARB, M. LELENTAL and C. A. THOMPSON, in "Magnetic Susceptibility of Superconductors and Other Spin System," edited by R. A. Hein, T. L. Francavilla and D. H. Liebenberg (Plenum Press, New York, 1991) pp. 49–80.

Received 23 July 1997
and accepted 5 May 1999